J Neurophysiol 119: 1924–1933, 2018.
First published February 14, 2018; doi:10.1152/jn.00524.2017.

RESEARCH ARTICLE | *Sensory Processing*

Neural correlates of economic value and valuation context: an event-related potential study

John Tyson-Carr,[1] Katerina Kokmotou,[1,2] Vicente Soto,[1] Stephanie Cook,[1] Nicholas Fallon,[1] Timo Giesbrecht,[3] and Andrej Stancak[1,2]

[1]*Department of Psychological Sciences, University of Liverpool, Liverpool, United Kingdom;* [2]*Institute for Risk and Uncertainty, University of Liverpool, Liverpool, United Kingdom; and* [3]*Unilever Research and Development, Port Sunlight, United Kingdom*

Submitted 11 July 2017; accepted in final form 6 February 2018

Tyson-Carr J, Kokmotou K, Soto V, Cook S, Fallon N, Giesbrecht T, Stancak A. Neural correlates of economic value and valuation context: an event-related potential study. *J Neurophysiol* 119: 1924–1933, 2018. First published February 14, 2018; doi: 10.1152/jn.00524.2017.—The value of environmental cues and internal states is continuously evaluated by the human brain, and it is this subjective value that largely guides decision making. The present study aimed to investigate the initial value attribution process, specifically the spatiotemporal activation patterns associated with values and valuation context, using electroencephalographic event-related potentials (ERPs). Participants completed a stimulus rating task in which everyday household items marketed up to a price of £4 were evaluated with respect to their desirability or material properties. The subjective values of items were evaluated as willingness to pay (WTP) in a Becker-DeGroot-Marschak auction. On the basis of the individual's subjective WTP values, the stimuli were divided into high- and low-value items. Source dipole modeling was applied to estimate the cortical sources underlying ERP components modulated by subjective values (high vs. low WTP) and the evaluation condition (value-relevant vs. value-irrelevant judgments). Low-WTP items and value-relevant judgments both led to a more pronounced N2 visual evoked potential at right frontal scalp electrodes. Source activity in right anterior insula and left orbitofrontal cortex was larger for low vs. high WTP at ~200 ms. At a similar latency, source activity in right anterior insula and right parahippocampal gyrus was larger for value-relevant vs. value-irrelevant judgments. A stronger response for low- than high-value items in anterior insula and orbitofrontal cortex appears to reflect aversion to low-valued item acquisition, which in an auction experiment would be perceived as a relative loss. This initial low-value bias occurs automatically irrespective of the valuation context.

NEW & NOTEWORTHY We demonstrate the spatiotemporal characteristics of the brain valuation process using event-related potentials and willingness to pay as a measure of subjective value. The N2 component resolves values of objects with a bias toward low-value items. The value-related changes of the N2 component are part of an automatic valuation process.

Becker-DeGroot-Marschak mechanism; insula; N2; orbitofrontal cortex; P2

Address for reprint requests and other correspondence: J. Tyson-Carr, Dept. of Psychological Sciences, Univ. of Liverpool, Liverpool L69 7ZA, UK (e-mail: hljtyson@liverpool.ac.uk).

INTRODUCTION

Economic values of stimuli are continuously and automatically encoded in the human brain. Previous brain imaging studies have shown that valuation occurs predominantly in the orbitofrontal cortex (OFC), the ventromedial prefrontal cortex (vmPFC), and the ventral striatum (Bartra et al. 2013; Clithero and Rangel 2014; Padoa-Schioppa 2007; Raghuraman and Padoa-Schioppa 2014).

Value attribution is one of the first stages of any value-based decision (Rangel et al. 2008). Previous studies investigated the modulation of event-related potential (ERP) components by hedonic aspects of visual stimuli (for a review, see Hajcak et al. 2012). For example, a negativity bias reflecting preferential processing of unpleasant stimuli may result in greater ERP responses (Delplanque et al. 2006; Huang and Luo 2006; Smith et al. 2003). Some studies identified the role of the late positive potential in the encoding of emotional stimulus valence (Foti et al. 2009; MacNamara et al. 2009; Moser et al. 2006); however, the late positive potential also varies as a function of motivational significance (i.e., salience; Weinberg and Hajcak 2010). Although the subjective pleasantness of a stimulus may contribute to the value of perceived goods, economic value is not identical to emotional valence.

Electrophysiological studies have highlighted that value-related signals appear as early as 200 ms after stimulus presentation in binary decision tasks where a choice between two options is required (Larsen and O'Doherty 2014; Tzovara et al. 2015). Differences in ERPs were also observed across multiple time windows ranging from 150 to 800 ms (Harris et al. 2011). However, ERPs were not investigated in relation to behavioral measures concerning economic value directly. Other investigations of the value-encoding phase were focused within specific brain regions (Hunt et al. 2012). A common finding in previous ERP studies investigating the representation of value-based preferences in binary reaction time tasks was a progression of activations from the occipito-temporal cortical regions to frontal and prefrontal sites over the course of the ERP (Harris et al. 2011; Larsen and O'Doherty 2014). However, the involvement of a reaction time response in experiments investigating the representation of value also adds a motor readiness component to ERPs that may interact with activations related to the automatic valuation process occurring in the absence of

  ISSN 0022-3077.

decision making (Gluth et al. 2013; Polanía et al. 2014). Furthermore, binary decision making compared with reporting hedonic ratings has been found to involve different brain regions, such as anterior cingulate cortex (Rolls et al. 2009).

Several ERP components relevant to value-based decision making have been revealed in previous literature. Event-related negativity and feedback-related negativity are two ERP components that, because of their nature, allow us to investigate decision making processes (Walsh and Anderson 2012). These two components are elicited by feedback after decision tasks and are relevant to reward-prediction errors (Gehring et al. 2012; Nieuwenhuis et al. 2004; Yu and Huang 2013). Additionally, the P300 ERP component is often implicated, in which the P300 encodes outcome valence (San Martín 2012; Yeung and Sanfey 2004). It is generally found that these ERP components are specific to outcome processing, although it has been revealed that the eliciting stimuli can modulate the ERP magnitude at the outcome stage (Yeung and Cohen 2006).

A common method for estimating the economic value of goods is via auction tasks such as the Becker-DeGroot-Marschak (BDM) mechanism (Becker et al. 1964). The BDM mechanism is an incentive-compatible method for estimating a subject's willingness to pay (WTP) for goods and prospects (Wilkinson and Klaes 2012). Previous functional magnetic resonance imaging (fMRI) studies have established that the brain valuation system activates during the BDM mechanism (Chib et al. 2009; Plassmann et al. 2007, 2010).

The context in which economic decisions are made can also influence the neural activations within the brain valuation system. For example, neural responses within valuation regions can be modulated during an auction task in which bids may be forced (Plassmann et al. 2007, 2010), passive viewing tasks (Levy et al. 2011), and tasks in which value is irrelevant (Grueschow et al. 2015; Polanía et al. 2014) or where outcomes are uncertain (Payzan-LeNestour et al. 2013). Activation of the brain valuation system during tasks in which it was not required demonstrates the automaticity of valuation processes (Lebreton et al. 2009).

The aim of the present study was to investigate the spatiotemporal aspects of brain economic evaluation of everyday household items during a task in which value was either task relevant or irrelevant. Subjects viewed each item but were not requested to make a speeded response; rather, they rated the likeability or the material features of the item. A BDM auction experiment was used to evaluate WTP in a separate session, and the WTP values were correlated with ERPs and subjective ratings.

METHODS

Participants. Twenty-five healthy participants (14 women, 11 men) with a mean age of 24 ± 4.67 (mean ± SD) yr took part in the study. The experimental procedures were approved by the Research Ethics Committee of the University of Liverpool. All participants gave written informed consent in accordance with the Declaration of Helsinki. Participants were reimbursed for their time and travel expenses.

Procedure. All experimental procedures were carried out in a dimly lit, sound-attenuated room. Participants sat in front of a 19-in. LCD monitor. The study was carried out in two sessions ~2–5 days apart. During the first session, participants completed the auction task. During the second session, participants completed the rating task. The stimuli comprised 90 everyday household items varying in value from £0.75 to £4.00 with a mean value of £2.52 ± £1.01 (mean ± SD) obtained from a shopping catalog. Food items were excluded to avoid confounds arising from difference in the appetitive value of stimuli between *session 1* and *session 2* of the study. Stimuli were presented in random order. Presentation of stimuli was controlled with Cogent 2000 (University College London, London, UK) in MATLAB 7.8 (MathWorks). Experimental protocols and stimulus timings are illustrated in Fig. 1.

Auction task. The protocol for the auction task was adapted from previous studies (Plassmann et al. 2007, 2010) and employed the BDM mechanism (Becker et al. 1964; Wilkinson and Klaes 2012). Each stimulus was presented once, resulting in a total of 90 auctions.

Each auction consisted of a fixation cross followed by an evaluation stage, a bidding period, and then feedback. During the evaluation stage, participants appraised the stimulus that was presented on-screen. The bidding period required the participants to bid on the item. Here, participants were asked to bid between £0 and £4 in increments of £0.50, giving a total of nine options. During the feedback stage, participants were notified as to whether or not the item was won. The outcome of an auction was dependent on the bid and a randomly generated number, in which the item was purchased when $b \geq r$, where b represents the bid and r represents the randomly generated number for that auction. At the end of the experiment, three auctions resulting in a purchase were selected at random. For each auction selected, a price equal to r was subtracted from an initial endowment of £12. Therefore, the actual endowment could vary between £0 and £12. The participant could pick up the items won within a few days of completion of the full experiment.

Rating task. Approximately 2–5 days after completion of the auction task, participants returned to take part in *session 2*. Electroencephalography (EEG) was recorded continuously with the 128-channel Geodesics EGI system (Electrical Geodesics, Eugene, OR) with the sponge-based HydroCel Sensor Net. The sensor net was aligned with respect to three anatomical landmarks (two preauricular points and the nasion). Electrode-to-skin impedances were kept below 50 kΩ and at equal levels across all electrodes, as recommended for the system (Ferree et al. 2001; Luu et al. 2003; Picton et al. 2000). The

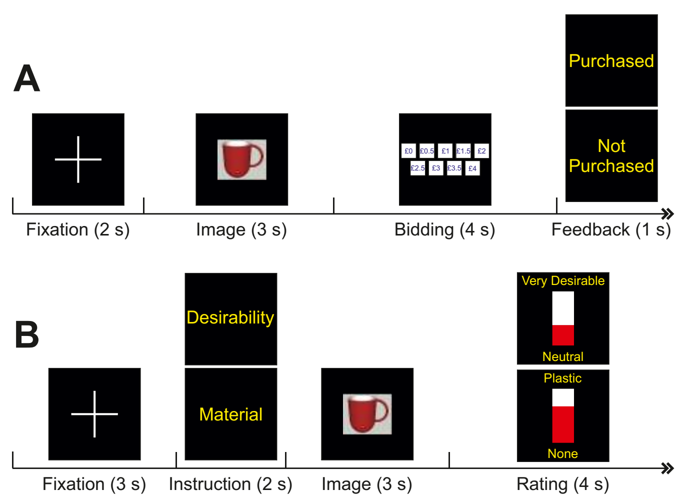

Fig. 1. Experimental protocol. *A*: timeline of auction task. A fixation cross was presented at the beginning of each trial for 2 s. After offset of the fixation cross, an image was presented for 3 s, followed by the bidding options for 4 s. A total of 9 options were available between £0 and £4 in increments of £0.50. After the selection of a bid, feedback was presented for 1 s to indicate the outcome of that auction. *B*: timeline of EEG task. A fixation cross was presented at the beginning of each trial for 3 s. Next, an instruction was presented for 2 s to indicate the demands of the trial, followed by an image for 3 s. After image offset, a visual analog scale was presented for 4 s to allow either a desirability rating or a material estimation depending on the preceding instruction.

sampling rate was 1,000 Hz, and Cz was used as the initial reference. Data were filtered online with a 0.1- to 200-Hz band-pass filter.

After the EEG cap was fitted, participants completed a computerized rating task. Each trial began with a fixation cross followed by an instruction stage, an evaluation period, and then rating. During the instruction stage, participants were presented with either of the words "DESIRABILITY" and "MATERIAL," which served to cue the participant to the required type of evaluation. The evaluation stage began with the presentation of one of the visual stimuli, followed by the presentation of a visual analog scale for the rating stage. In the value-relevant condition the participant would have to rate the desirability of the preceding stimulus (anchors: "neutral"–"very desirable"), while in the value-irrelevant condition the participant would rate the proportion of the preceding stimulus composed of a certain material (for example, "none"–"plastic"). Here, the proportion of the scale that is shaded indicates the percentage of plastic composition. Desirability and material estimation trials were randomly intermixed within blocks.

Investigating the neural basis of subjective value is complicated by the multiple nonspecific neural processes elicited during experimental paradigms used to reveal subjective value. During the rating task, the only difference between these two conditions was the calculation of subjective value for the trials in which desirability was rated. Any differences in ERPs between these two trials can therefore be attributed to computation required to report subjective value. Of course, automatic processes involved in valuation would still be present. Each stimulus was presented in both conditions, yielding a total of 180 trials, split into three blocks.

Median split of WTP values. The stimulus set was divided into high- and low-WTP items with a median split of subjective values. In the case of items with identical value on both sides of the split, the items with that value were removed in such a manner that there was no overlap in value between the two sides and there was an equal number of stimuli in each category. For an unequal number of stimuli of identical value on each side of the split, stimuli of that value were removed randomly from the side with more. This produced two categories of stimuli (high and low value) of equal size for each participant, with a mean of 38.48 ± 5.02 (mean ± SD) items remaining in each condition.

ERP analysis. EEG data were preprocessed with the BESA v. 6.0 program (MEGIS, Munich, Germany). Oculographic artifacts and electrocardiographic artifacts were removed with principal component analysis based on averaged eyeblinks and artifact topographies (Berg and Scherg 1994). Data were also visually inspected for the presence of atypical electrode artifacts due to muscle movement. Data were filtered from 1 to 45 Hz, and epochs contaminated with artifacts were excluded manually.

ERPs in response to stimulus presentation were computed separately for each level within conditions (high-value item and desirability rating; high-value item and material estimation; low-value item and desirability rating; low-value item and material estimation) by averaging respective epochs in the intervals ranging from 300 ms before image onset to 1,000 ms after image onset. Epochs were baseline corrected using a time window of −300 to 0 ms relative to stimulus onset. The mean number of accepted trials in each condition (after the median split and artifact rejection) was 32.4 ± 5.8 (mean ± SD).

Source dipole reconstruction. Grand average potentials were computed by combining all conditions. The grand average waveform was used to define a source dipole model in the BESA v. 6.0 program. With a sequential strategy (Hoechstetter et al. 2001; Stancak et al. 2002), equivalent current dipoles (ECDs) were fitted to describe the three-dimensional source currents in the regions contributing predominantly to the data (Scherg and Von Cramon 1986). Six ECDs were consecutively seeded until the source mode explained 91.6% of the variance. This amount of explained variance is comparable to previous ERP source dipole localization studies (Hämäläinen et al. 1993; Schlereth et al. 2003; Stancak et al. 2012; Vrána et al. 2005) and suggests that the six-dipole model explained all major ERP components. Classical LORETA analysis recursively applied (CLARA) method, which is an iterative application of the LORETA algorithm (Pascual-Marqui et al. 1994), was used as an independent source localization method to confirm the locations of the ECDs (Wright et al. 2015). The orientations of ECDs were fitted with the constraint of fixed dipole locations and determined at the maximum of the source strength. A four-shell ellipsoid head volume conductor model was employed, using the following conductivities: brain = 0.33 S/m; scalp = 0.33 S/m; bone = 0.0042 S/m; cerebrospinal fluid = 1 S/m.

Source waveforms for each condition were exported and analyzed with the EEGLAB toolbox (Delorme and Makeig 2004). Because of the large number of statistical tests that this requires, P values were corrected with permutation-based repeated-measures ANOVA utilizing 5,000 permutations (Maris and Oostenveld 2007). For each latency identified, mean activation over a 10-ms period was calculated, centered on the peak of the observed effect and for each participant. The data were exported to SPSS Statistics version 22.0 (IBM, 2013) for further analysis.

It is important to note the limitations of source analysis techniques due to the inverse problem manifesting in the possibility of generating a number of plausible source dipole models (Michel and Murray 2012). Therefore, a priori information, such as constraining the source dipole locations to the cortical mantle, has been implemented in source dipole localization methods to reduce the number of possible solutions (Michel et al. 2004). To build a plausible source dipole model, we applied two different source dipole modeling methods: first, the sequential method consisting of fitting equivalent current dipoles sequentially and second, a distributed source dipole modeling method (CLARA). Both methods yielded highly convergent source dipole models, which mitigates but does not completely overcome the limitations associated with the large number of potential source dipole solutions given the mathematical features of the inverse problem.

RESULTS

Behavioral data. The high-value items had a mean WTP of 2.1 ± 0.87 (mean ± SD) and a desirability rating of 50.4 ± 29.7, whereas the low-value items had a mean WTP of 0.66 ± 0.62 and a desirability rating of 27 ± 25.3. To ensure that this finding was not confounded by individual differences, a regression model for each participant was created with WTP as a predictor and desirability as a dependent variable. This produced a mean unstandardized coefficient of 15.5 ± 9.37; a one-sample t-test revealed this to be significantly different from zero [$t(24) = 8.27$, $P < 0.001$]. A mean adjusted R^2 of 0.23 ± 0 0.17 (mean ± SD) was also found across subjects. Therefore, desirability of objects was linearly related to WTP (see Fig. 2).

Source dipole model. Figure 3 illustrates the ERPs at each electrode site in response to stimulus presentation across all conditions in the form of a butterfly plot; ERP components and their corresponding latencies and topographies are labeled. Four distinct ERP components were observed across the epoch beginning with the visually evoked P1 component peaking at 99 ms, a component related to the early processing of visual stimuli (Hopf et al. 2002) and characterized by strong positivity over the central occipital electrodes with reversed polarity over the frontal electrodes. A P2 component peaked at 209 ms with bilateral positivity over the occipital electrodes but with negativity restricted over a frontal region on the right side of the head (Freunberger et al. 2007; Luck 2005). Although clearly overlapping with the P2, the N2 component peaking at

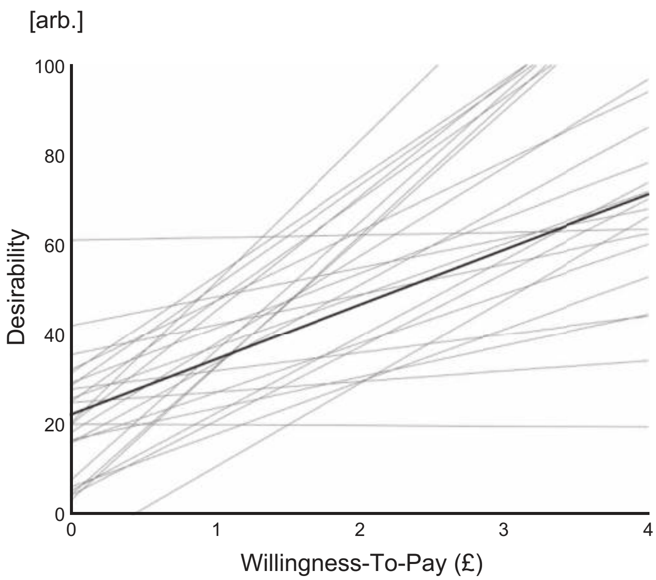

Fig. 2. Regression lines for each subject predicting desirability from WTP. Grand average regression line is shown in black.

243 ms can be differentiated by the additional negativity over a frontal region (Folstein and Van Petten 2008). The P3 component (Polich 2007) emerges at ~316 ms in a parietal region on the right side of the scalp before reaching a positive maximum at 354 ms over the midline frontal electrodes.

Figure 4*A* shows the source waveforms and the appropriate topographic maps for different ECDs, and Fig. 4*B* illustrates the spatial localization of the ECDs. *ECD1* was located in the right LG (Brodmann area 18; approximate Talairach coordinates: $x = 18$ mm, $y = -59$ mm, $z = 9$ mm), with a peak latency at 95 ms and again at 121 ms. *ECD2* showed similar characteristics, being located in the left LG (Brodmann area 18; $x = -17$ mm, $y = -59$ mm, $z = 9$ mm) with a peak latency at both 100 ms and 215 ms. Both *ECD1* and *ECD2* showed a positive maximum over the medial occipital electrodes and a negative potential over a frontal region of the scalp. The latency and the topographical pattern indicate that these two sources were equivalent to the visual P1 component. *ECD3* was located in the right anterior insula cortex (AIC) (Brodmann area 13; $x = 32$ mm, $y = 15$ mm, $z = 0$ mm), peaking at 233 ms and showing maximum negativity over a frontal region on the right side of the scalp. This spatial map corresponds to the frontal portion of the N2 component. *ECD4* was located in the left OFC (Brodmann area 11; $x = -26$ mm, $y = 34$ mm, $z = -2$ mm), showing a small peak at 230 ms. *ECD4* projected positivity over a frontal region localized marginally on the left side. However, this was masked by the N2 component. *ECD5* was located in the right parahippocampal gyrus (PHG) (Brodmann area 28; $x = 19$ mm, $y = -17$ mm, $z = -21$ mm), showing two peak latencies of 215 ms and 316 ms corresponding to both the P2 and the early P3 component. *ECD5* accounted for positivity over a posterior region, localized primarily on the right side of the scalp. *ECD6* was fitted in the posterior cingulate cortex (PCC) (bordering closely with the anterior cingulate cortex; Brodmann area 31; $x = 3$ mm, $y = -18$ mm, $z = 42$ mm). The source peaked at 248 ms and 431 ms, with negativity being distributed across a frontal region of the scalp at 248 ms (contributing to the N2 component at the vertex) and positivity at 431 ms. The final source dipole model accounted for 91.6% of the total variance. CLARA method was used to verify the origins of the fitted ECDs. A mean discrepancy of ~15 mm was found between the location of each ECD and the maxima of the nearest cluster.

Effects of rating task and WTP. To test the effect of rating task and value on ERPs, a two-way ANOVA for repeated measures was carried out over the latency interval ranging from −200 ms to 450 ms using permutation analysis (Maris and Oostenveld 2007) with 5,000 permutations. The *F*-value

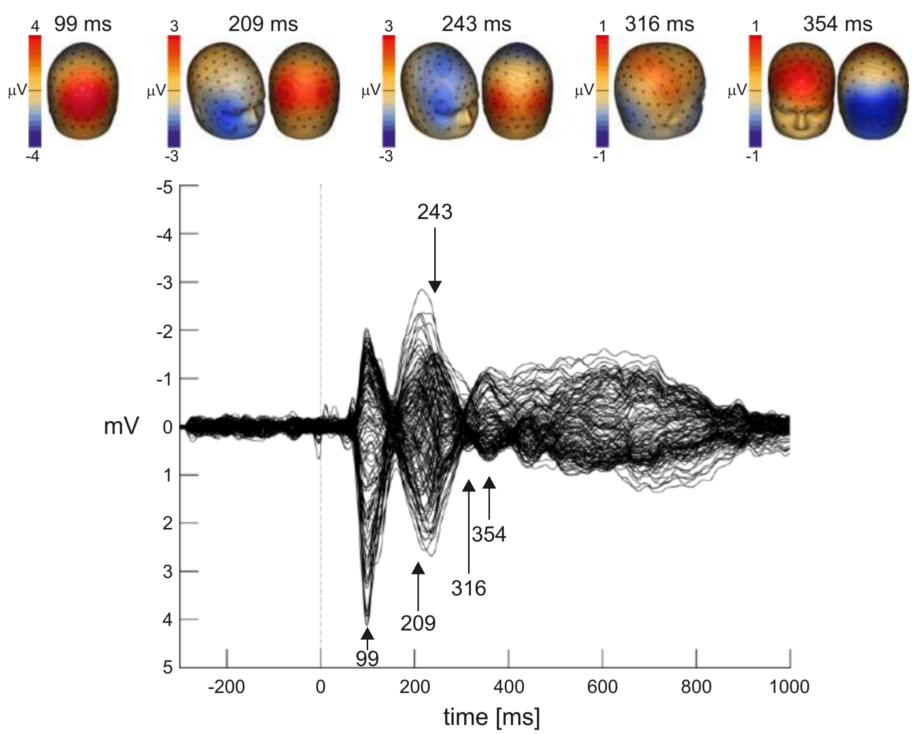

Fig. 3. Butterfly plot of grand average ERPs in response to stimulus presentation. Distinct ERP components are highlighted with arrows (99, 209, 243, 316, and 354 ms). The topographic map for each ERP component is also displayed.

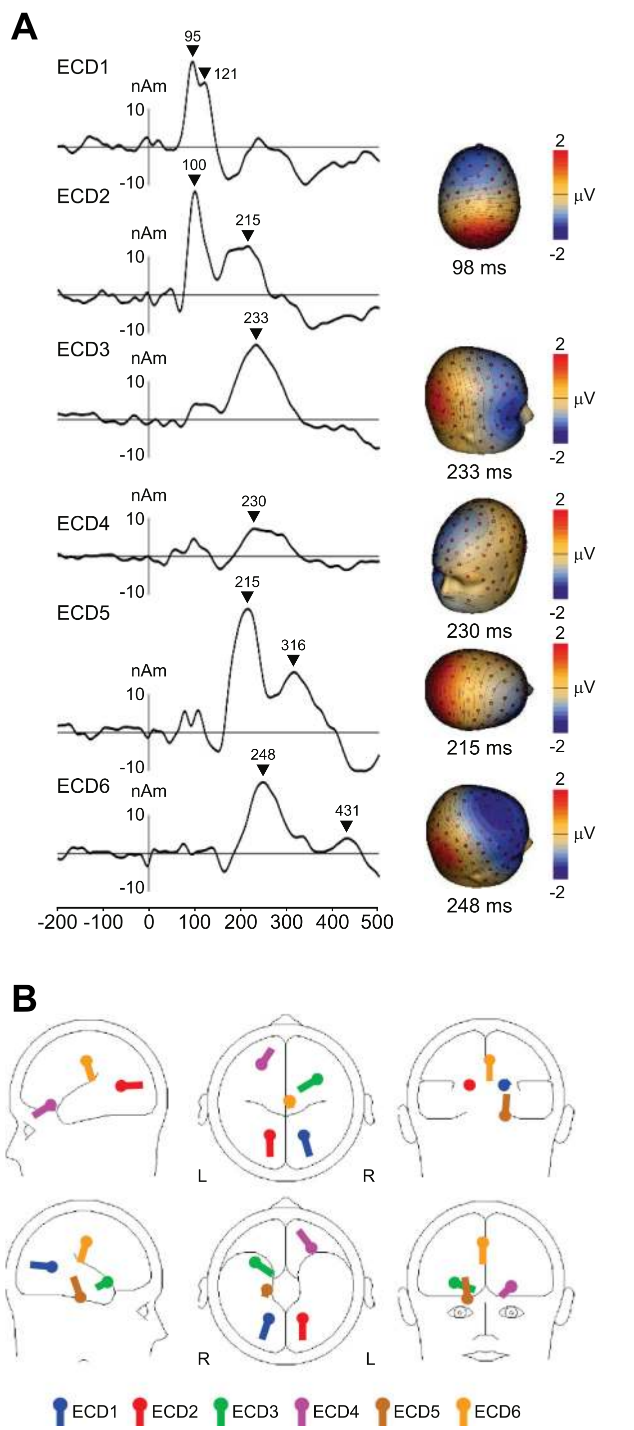

Fig. 4. Source dipole model of ERPs. *A*: source dipole waveforms in 6 ECDs. Peak latencies and the topographic maps for each of the ECDs are shown. *B*: locations and orientations of the 6 ECDs in the schematic glass brain.

waveforms were masked inclusively to highlight significant latencies that extended beyond three standard deviations of the source's mean baseline amplitude. Figure 4 shows the topographies at the peak significance of each observed main effect with the corresponding source waveform. Activity over a 10-ms interval centered on the peak significance for each effect (indicated by the shaded region on the source waveform) was exported for further analysis. Table 1 and Table 2 summarize the mean amplitude and test statistics for each condition over the stated time interval for the main effects of rating task (desirability vs. material) and value (high vs. low); significant interactions are highlighted in Table 3.

Table 1. *Mean source amplitude for desirability and material estimation conditions for each significant latency and corresponding ECD*

ECD	Time Interval, ms	Desirability	Material	$F_{(24)}$	P
ECD2	172–182	14.2 ± 23.2	9.32 ± 22.3	9.93	0.004
ECD3	201–211	19.28 ± 14.51	12.04 ± 12.2	17.6	<0.001
ECD5	204–214	37.26 ± 20.81	27.49 ± 20.09	8.34	0.008

Values are mean ± SD source amplitudes for desirability and material estimation conditions over the stated time interval for each significant latency and the corresponding ECD. *F* and *P* values for the relevant ANOVA are also displayed.

Figure 5*A* indicates three significant main effects of rating task on the activity from *ECD2*, *ECD3*, and *ECD5*. The waveforms for these ECDs all demonstrate larger activation for desirability ratings than for material estimation ratings. Figure 5*B* illustrates the two significant main effects of value on the activity from *ECD3* and *ECD4*, each displaying greater activation for low-value items. Despite the main effect of value at 233 ms in *ECD4*, it is important to note the difficulty in discerning the differences on scalp topographies because of the dominance of the negativity originating from *ECD3*, which peaked at approximately the same time. Only one significant interaction between rating task and value was observed (*ECD6*), which is visualized in Fig. 5*C*. During the value rating condition, source activation for a desirability rating of a high-value item was higher than in other conditions. Pairwise comparisons indicate that this activation was significantly stronger than during the material estimation and high value condition [$t(24) = 2.23$, $P = 0.035$] and also the desirability rating and low value condition [$t(24) = 2.1$, $P = 0.046$] but not the material estimation and low value condition [$t(24) = 0.65$, $P = 0.524$]. No other significant differences were found ($P > 0.05$).

A possible explanation for this interaction could be a result of task-switching. For example, upon presentation of a high-value item, participants would need to suppress their response if the task required material estimation with a low composition of the given material, with the same going for a low-value item in the material estimation task in which composition was high. To test this, a regression model was produced for each subject with desirability as the independent variable and material composition as the dependent variable. This produced a mean unstandardized coefficient of −0.063, which was not significantly different from zero [$t(24) = -1.51$, $P = 0.145$], thus suggesting that task-switching does not adequately explain the interaction effect in PCC.

Table 2. *Mean source amplitude for high- and low-value conditions for each significant latency and corresponding ECD*

ECD	Time Interval, ms	High Value	Low Value	$F_{(24)}$	P
ECD3	195–205	10.07 ± 12.85	17.81 ± 15.31	9.19	0.006
ECD4	228–238	5.09 ± 8.07	9.36 ± 8.89	12.57	0.002

Values are mean ± SD source amplitudes for high- and low-value conditions over the stated time interval for each significant latency and the corresponding ECD. *F* and *P* values for the relevant ANOVA are also displayed.

Table 3. *Mean source amplitude for desirability and material estimation ratings of high- and low-value items for each significant latency and corresponding ECD*

ECD	Time Interval, ms	HD	HM	LD	LM	$F_{(24)}$	*P*
ECD6	424–434	7.44 ± 12.76	1.85 ± 10.13	1.47 ± 10.32	5.05 ± 15.2	8.25	0.008

Values are mean ± SD source amplitudes for desirability ratings of high (HD)- and low (LD)-value items and for material estimation ratings of high (HM)- and low (LM)-value items for each significant latency and the corresponding ECD over the stated time interval. *F* and *P* values for the relevant ANOVA are also displayed.

DISCUSSION

This study explored the cortical representation of value by comparing items associated with high or low WTP and recorded ERPs during passive viewing of items in two different valuation contexts, allowing us to disentangle the automatic and the elaborate and conscious valuation processes. Results showed increased cortical activity following the presentation of low-value stimuli at the latency of ~200 ms, corresponding to the N2 and P2 components of ERPs. Although multiple sources contributed to ERP data at this latency, the economic value of items only modulated the activation in the right AIC and the left OFC. The effects of valuation context were seen in the left lingual gyrus (LG), right AIC, and right PHG.

Modulation of source activity within the right AIC peaked at 200 ms, and activity was the strongest for rating of low-value items. Although overlapping with the P2 component, source dipole orientation and topographical differences in the negativity over the forehead indicated that the N2 component that demonstrated an effect of value was distinct from the P2 component. The N2 potential was previously reported as being related to aspects of attentional selection (Codispoti et al. 2006; Näätänen and Picton 1986; Patel and Azzam 2005) or emotional content of visual stimuli (Olofsson and Polich 2007). The anterior N2 component has been related more specifically to novelty detection and cognitive control (Folstein and Van Petten 2008). The present study shows that the right AIC, a region known to be involved together with the OFC and amygdala in loss aversion (Canessa et al. 2013, 2017; Markett et al. 2016; Tom et al. 2007), contributed to effects of economic value on the amplitude of the N2 component. Therefore, it is possible that the bias toward low-value items reflects a loss-averse response, as low-value items could represent possible sources of financial loss. However, without more experimental control it is difficult to speculate on the underlying cognitive processes.

The low-value bias seen in the N2 component might have been boosted in the present study by the relatively limited range of value among the items on offer. Bartra et al. (2013) report a quadratic pattern within the AIC showing increased BOLD signal in response to extreme outcomes, positive or negative, and decreased BOLD for neutral stimuli. With a relatively small range of values in the present study (£0–£4), the low-value items may well have been negatively encoded (high arousal). In contrast, the high-value items may not have passed a threshold to be perceived as truly rewarding, thus eliciting no arousal response.

A similar low-value bias was also seen in left OFC at a latency of 233 ms; despite falling within the N2 component latency, this effect was characterized by increased positivity over the left frontal region but masked by the negativity of the N2. The modulation of source activity for this ECD by stimulus value exhibits an automatic valuation, independent of the valuation context. Modulation of BOLD signal by subjective value has been observed frequently, often within the OFC (Clithero and Rangel 2014). Interestingly, this modulation has been observed for various paradigms utilizing several measures of value such as hedonicity ratings (Grabenhorst and Rolls 2009; Lebreton et al. 2009), binary choice tasks (FitzGerald et al. 2009), and, importantly, BDM auctions (Plassmann et al. 2007, 2010). The same modulation is also found for multiple reward types and across multiple stages of the decision making process (for a review, see Peters and Büchel 2010). Further to this, animal research utilizing electrophysiological methods has highlighted the encoding of subjective value within the OFC (Padoa-Schioppa 2013; Padoa-Schioppa and Assad 2006). Similar conclusions have been drawn regarding the vmPFC (Bartra et al. 2013; Clithero and Rangel 2014); however, given the limitations to spatial resolution that EEG presents, the present findings may not differentiate the activation of the OFC from the neighboring vmPFC. The emergence of value-based signals in electrophysiological animal research has been observed in OFC at latencies as early as 150 ms (Padoa-Schioppa 2013). Thus formation of subjective value occurs automatically at an early stage and aids subsequent decision, regardless of whether this signal is an accurate depiction of the ultimate value assigned to the stimulus after further deliberation. However, given the task order in the present study, it is important to recognize the potential role that memory may have played in producing this automatic valuation. The auction task always preceded the stimulus rating task, resulting in participants having already reported their valuation of each of the stimuli. Although the time between the two tasks was between 2 and 5 days, it is possible that the valuation of the stimuli before the EEG task may have contributed to this finding because of memories originating from the auction task.

The cortical activity in the 200-ms latency range was also modulated by the valuation context. Given that the only computational difference between the two rating tasks is the presence of valuation, any differences in ERPs between the two contexts likely represent the cortical responses associated with attribution of value. The first modulation by the context was observed within the latency of the P2 component at 177 ms; the source activity in the LG was stronger when subjects focused on desirability of items rather than the material compositions. It has been suggested that the P2 is involved in working memory processes (Finnigan et al. 2011; Lefebvre et al. 2005; Taylor et al. 1990; Wolach and Pratt 2001), visual feature recognition (Hillyard and Münte 1984), and attention allocation (Martín-Loeches et al. 1997). Federmeier and Kutas (2002) reported context-dependent modulations of the P2 in the left hemisphere, which finding accords with the present study.

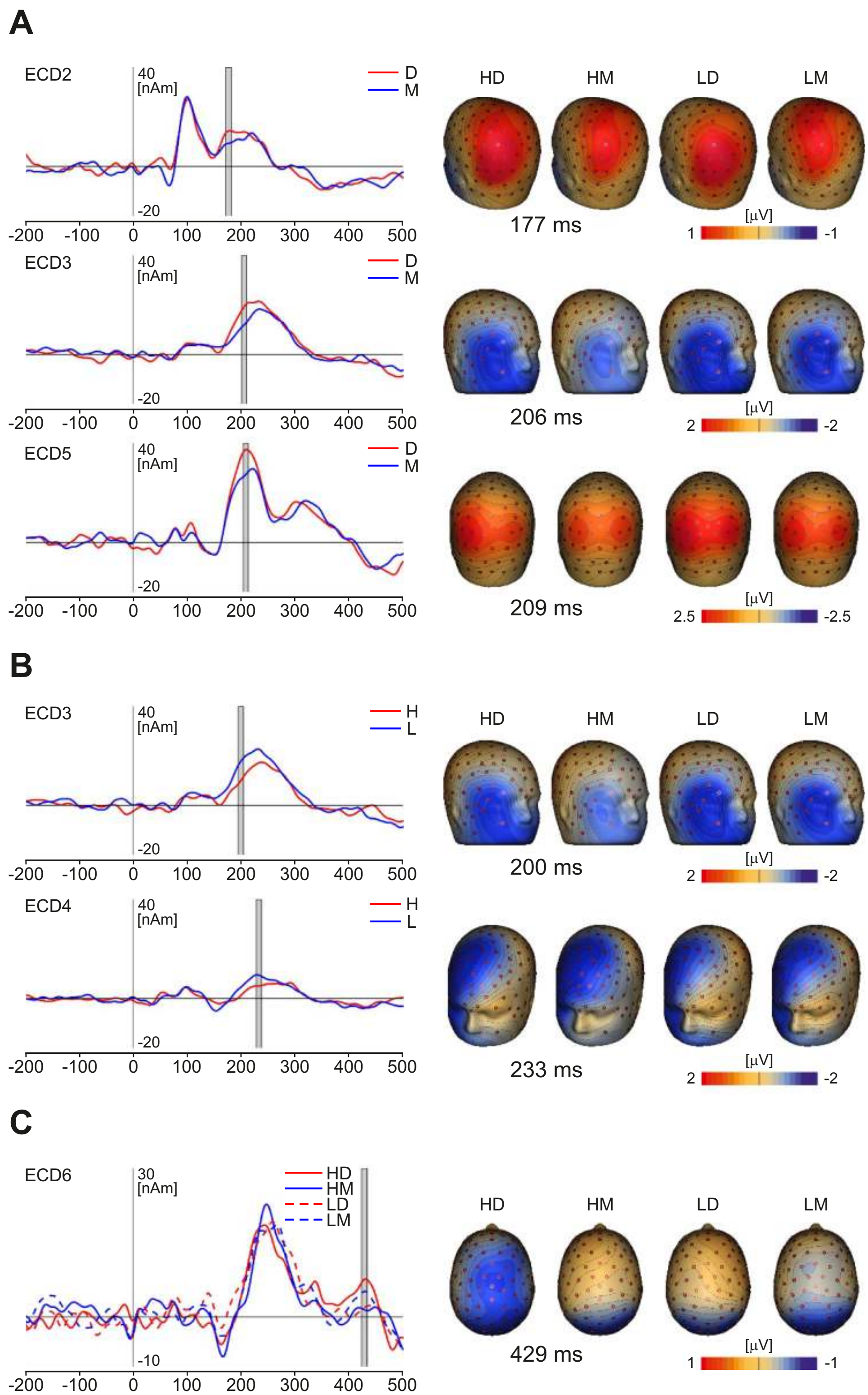

Fig. 5. Effects of subjective value and context on source dipole waveforms. Each line represents the source dipole waveform for each condition [D, desirability rating; M, material estimation; H, high-value items; L, low-value items; desirability of high (HD)- and low (LD)-value items; material estimation of high (HM)- and low (LM)-value items]. Gray shaded region on the source dipole waveforms indicates a 10-ms latency period in which a main effect or interaction was revealed, centered on the peak significance. Topographic maps for each condition are displayed. *A*: ECDs demonstrating a main effect of rating task (*ECD2*, *ECD3*, and *ECD5*). *B*: ECDs demonstrating a main effect of value (*ECD3* and *ECD4*). *C*: ECD demonstrating significant interaction between rating task and value (*ECD6*).

An effect of the valuation context was also observed in the P2 component at a slightly later latency of 209 ms. This modulation was related to an increase in source activity in right PHG when evaluating the desirability of items compared with evaluating materials. Given the role of the PHG in memory processes (Aminoff et al. 2013), it is likely here that focusing on the desirability of a stimulus has elicited working memory processes to a greater extent, or required a greater magnitude of attentional allocation. This may be due to the more complex analysis required to reach a decision about value rather than a more simple perceptual evaluation. Assuming that value-based decisions require an in-depth analysis of the stimuli, in contrast to the perceptual decision requiring estimation of a single material, this modulation may simply be a result of visual feature recognition regarding multiple aspects of the stimuli (Hillyard and Münte 1984).

Finally, the right AIC also showed an increased source activity for the rating of desirability, resulting in greater negativity over the right forehead. Augmentation of anterior N2 components has been attributed to attentional processes (Codispoti et al. 2006; Näätänen and Picton 1986; Patel and Azzam 2005), and it seems the differing computational demands of the value-based and perceptual decisions augmented the observed N2 in the present study. The additional requirement of value computation for the value-based decision could be the contributing factor to this increased amplitude. Indeed, Näätänen and Picton (1986) highlight that the N2 component can be modulated by conscious processing of stimuli, and thus this processing may well be value specific.

A final modulation of ERPs by the valuation context was observed at ~429 ms in PCC. The source activity in PCC, manifested as the negative potential at vertex electrodes, was prominent for the rating of desirability of high-value items, indicating that this activation is specific to highly valued stimuli in an economically relevant context. However, this finding should be interpreted with caution because of the lack of statistically significant differences between the desirability rating of high-value items condition and the material estimation of low-value items at the same latency.

To conclude, we show that the subjective value of simple household items, measured as WTP in an auction experiment, manifests in ERPs in the latency window and electrodes corresponding to the N2 component. The value-related cortical response, purportedly originating in right AIC and left OFC, is enhanced for low-value items, possibly by eliciting loss aversion. The low-value bias in these cortical regions occurred across two different valuation contexts, suggesting that this response is a part of an automatic valuation process. In contrast to the subjective value, the valuation context modulates the P2 and N2 components with stronger cortical responses in left LG, right AIC, and right PHG occurring while subjects focused on desirability than on material aspects of items.

ACKNOWLEDGMENTS

We are grateful to Julia Jones and Hannah Roberts for assisting with technical aspects of the study.

GRANTS

This work was supported by a CASE studentship from the Economic and Social Research Council (Grant No. ES/J500094/1), with additional support from Unilever Research and Development.

DISCLOSURES

No conflicts of interest, financial or otherwise, are declared by the authors.

AUTHOR CONTRIBUTIONS

J.A.T.-C. and A.S. conceived and designed research; J.A.T.-C., K.K., V.S., S.C., and N.B.F. performed experiments; J.A.T.-C. and A.S. analyzed data; J.A.T.-C. and A.S. interpreted results of experiments; J.A.T.-C. and A.S. prepared figures; J.A.T.-C. and A.S. drafted manuscript; J.A.T.-C., K.K., V.S., S.C., N.B.F., T.G., and A.S. edited and revised manuscript; J.A.T.-C., K.K., V.S., S.C., N.B.F., T.G., and A.S. approved final version of manuscript.

REFERENCES

Aminoff EM, Kveraga K, Bar M. The role of the parahippocampal cortex in cognition. *Trends Cogn Sci* 17: 379–390, 2013. doi:10.1016/j.tics.2013.06.009.

Bartra O, McGuire JT, Kable JW. The valuation system: a coordinate-based meta-analysis of BOLD fMRI experiments examining neural correlates of subjective value. *Neuroimage* 76: 412–427, 2013. doi:10.1016/j.neuroimage.2013.02.063.

Becker GM, DeGroot MH, Marschak J. Measuring utility by a single-response sequential method. *Behav Sci* 9: 226–232, 1964. doi:10.1002/bs.3830090304.

Berg P, Scherg M. A multiple source approach to the correction of eye artifacts. *Electroencephalogr Clin Neurophysiol* 90: 229–241, 1994. doi:10.1016/0013-4694(94)90094-9.

Canessa N, Crespi C, Baud-Bovy G, Dodich A, Falini A, Antonellis G, Cappa SF. Neural markers of loss aversion in resting-state brain activity. *Neuroimage* 146: 257–265, 2017. doi:10.1016/j.neuroimage.2016.11.050.

Canessa N, Crespi C, Motterlini M, Baud-Bovy G, Chierchia G, Pantaleo G, Tettamanti M, Cappa SF. The functional and structural neural basis of individual differences in loss aversion. *J Neurosci* 33: 14307–14317, 2013. doi:10.1523/JNEUROSCI.0497-13.2013.

Chib VS, Rangel A, Shimojo S, O'Doherty JP. Evidence for a common representation of decision values for dissimilar goods in human ventromedial prefrontal cortex. *J Neurosci* 29: 12315–12320, 2009. doi:10.1523/JNEUROSCI.2575-09.2009.

Clithero JA, Rangel A. Informatic parcellation of the network involved in the computation of subjective value. *Soc Cogn Affect Neurosci* 9: 1289–1302, 2014. doi:10.1093/scan/nst106.

Codispoti M, Ferrari V, Junghöfer M, Schupp HT. The categorization of natural scenes: brain attention networks revealed by dense sensor ERPs. *Neuroimage* 32: 583–591, 2006. doi:10.1016/j.neuroimage.2006.04.180.

Delorme A, Makeig S. EEGLAB: an open source toolbox for analysis of single-trial EEG dynamics including independent component analysis. *J Neurosci Methods* 134: 9–21, 2004. doi:10.1016/j.jneumeth.2003.10.009.

Delplanque S, Silvert L, Hot P, Rigoulot S, Sequeira H. Arousal and valence effects on event-related P3a and P3b during emotional categorization. *Int J Psychophysiol* 60: 315–322, 2006. doi:10.1016/j.ijpsycho.2005.06.006.

Federmeier KD, Kutas M. Picture the difference: electrophysiological investigations of picture processing in the two cerebral hemispheres. *Neuropsychologia* 40: 730–747, 2002. doi:10.1016/S0028-3932(01)00193-2.

Ferree TC, Luu P, Russell GS, Tucker DM. Scalp electrode impedance, infection risk, and EEG data quality. *Clin Neurophysiol* 112: 536–544, 2001. doi:10.1016/S1388-2457(00)00533-2.

Finnigan S, O'Connell RG, Cummins TD, Broughton M, Robertson IH. ERP measures indicate both attention and working memory encoding decrements in aging. *Psychophysiology* 48: 601–611, 2011. doi:10.1111/j.1469-8986.2010.01128.x.

FitzGerald TH, Seymour B, Dolan RJ. The role of human orbitofrontal cortex in value comparison for incommensurable objects. *J Neurosci* 29: 8388–8395, 2009. doi:10.1523/JNEUROSCI.0717-09.2009.

Folstein JR, Van Petten C. Influence of cognitive control and mismatch on the N2 component of the ERP: a review. *Psychophysiology* 45: 152–170, 2008. doi:10.1111/j.1469-8986.2007.00602.x.

Foti D, Hajcak G, Dien J. Differentiating neural responses to emotional pictures: evidence from temporal-spatial PCA. *Psychophysiology* 46: 521–530, 2009. doi:10.1111/j.1469-8986.2009.00796.x.

Freunberger R, Klimesch W, Doppelmayr M, Höller Y. Visual P2 component is related to theta phase-locking. *Neurosci Lett* 426: 181–186, 2007. doi:10.1016/j.neulet.2007.08.062.

Gehring W, Liu Y, Orr JM, Carp J. The error-related negativity (ERN/Ne). In: *The Oxford Handbook of Event-Related Potential Components*, edited by Luck SJ, Kappenman ES. New York: Oxford Univ. Press, 2012, p. 231–294.

Gluth S, Rieskamp J, Büchel C. Classic EEG motor potentials track the emergence of value-based decisions. *Neuroimage* 79: 394–403, 2013. doi:10.1016/j.neuroimage.2013.05.005.

Grabenhorst F, Rolls ET. Different representations of relative and absolute subjective value in the human brain. *Neuroimage* 48: 258–268, 2009. doi:10.1016/j.neuroimage.2009.06.045.

Grueschow M, Polania R, Hare TA, Ruff CC. Automatic versus choice-dependent value representations in the human brain. *Neuron* 85: 874–885, 2015. doi:10.1016/j.neuron.2014.12.054.

Hajcak G, Weinberg A, MacNamara A, Foti D. ERPs and the study of emotion. In: *The Oxford Handbook of Event-Related Potential Components*, edited by Luck SJ, Kappenman ES. New York: Oxford Univ. Press, 2012, p. 441–472.

Hämäläinen M, Hari R, Ilmoniemi RJ, Knuutila J, Lounasmaa OV. Magnetoencephalography—theory, instrumentation, and applications to noninvasive studies of the working human brain. *Rev Mod Phys* 65: 413–497, 1993. doi:10.1103/RevModPhys.65.413.

Harris A, Adolphs R, Camerer C, Rangel A. Dynamic construction of stimulus values in the ventromedial prefrontal cortex. *PLoS One* 6: e21074, 2011. doi:10.1371/journal.pone.0021074.

Hillyard SA, Münte TF. Selective attention to color and location: an analysis with event-related brain potentials. *Percept Psychophys* 36: 185–198, 1984. doi:10.3758/BF03202679.

Hoechstetter K, Rupp A, Stancák A, Meinck HM, Stippich C, Berg P, Scherg M. Interaction of tactile input in the human primary and secondary somatosensory cortex—a magnetoencephalographic study. *Neuroimage* 14: 759–767, 2001. doi:10.1006/nimg.2001.0855.

Hopf JM, Vogel E, Woodman G, Heinze HJ, Luck SJ. Localizing visual discrimination processes in time and space. *J Neurophysiol* 88: 2088–2095, 2002. doi:10.1152/jn.2002.88.4.2088.

Huang YX, Luo YJ. Temporal course of emotional negativity bias: an ERP study. *Neurosci Lett* 398: 91–96, 2006. doi:10.1016/j.neulet.2005.12.074.

Hunt LT, Kolling N, Soltani A, Woolrich MW, Rushworth MF, Behrens TE. Mechanisms underlying cortical activity during value-guided choice. *Nat Neurosci* 15: 470–476, 2012. doi:10.1038/nn.3017.

Larsen T, O'Doherty JP. Uncovering the spatio-temporal dynamics of value-based decision-making in the human brain: a combined fMRI-EEG study. *Philos Trans R Soc Lond B Biol Sci* 369: 20130473, 2014. doi:10.1098/rstb.2013.0473.

Lebreton M, Jorge S, Michel V, Thirion B, Pessiglione M. An automatic valuation system in the human brain: evidence from functional neuroimaging. *Neuron* 64: 431–439, 2009. doi:10.1016/j.neuron.2009.09.040.

Lefebvre CD, Marchand Y, Eskes GA, Connolly JF. Assessment of working memory abilities using an event-related brain potential (ERP)-compatible digit span backward task. *Clin Neurophysiol* 116: 1665–1680, 2005. doi:10.1016/j.clinph.2005.03.015.

Levy I, Lazzaro SC, Rutledge RB, Glimcher PW. Choice from non-choice: predicting consumer preferences from blood oxygenation level-dependent signals obtained during passive viewing. *J Neurosci* 31: 118–125, 2011. doi:10.1523/JNEUROSCI.3214-10.2011.

Luck SJ. *An Introduction to the Event-Related Potential Technique*. Cambridge, MA: MIT Press, 2005.

Luu P, Tucker DM, Derryberry D, Reed M, Poulsen C. Electrophysiological responses to errors and feedback in the process of action regulation. *Psychol Sci* 14: 47–53, 2003. doi:10.1111/1467-9280.01417.

MacNamara A, Foti D, Hajcak G. Tell me about it: neural activity elicited by emotional pictures and preceding descriptions. *Emotion* 9: 531–543, 2009. doi:10.1037/a0016251.

Maris E, Oostenveld R. Nonparametric statistical testing of EEG- and MEG-data. *J Neurosci Methods* 164: 177–190, 2007. doi:10.1016/j.jneumeth.2007.03.024.

Markett S, Heeren G, Montag C, Weber B, Reuter M. Loss aversion is associated with bilateral insula volume. A voxel based morphometry study. *Neurosci Lett* 619: 172–176, 2016. doi:10.1016/j.neulet.2016.03.029.

Martín-Loeches M, Schweinberger SR, Sommer W. The phonological loop model of working memory: an ERP study of irrelevant speech and phonological similarity effects. *Mem Cognit* 25: 471–483, 1997. doi:10.3758/BF03201123.

Michel CM, Murray MM. Towards the utilization of EEG as a brain imaging tool. *Neuroimage* 61: 371–385, 2012. doi:10.1016/j.neuroimage.2011.12.039.

Michel CM, Murray MM, Lantz G, Gonzalez S, Spinelli L, Grave de Peralta R. EEG source imaging. *Clin Neurophysiol* 115: 2195–2222, 2004. doi:10.1016/j.clinph.2004.06.001.

Moser JS, Hajcak G, Bukay E, Simons RF. Intentional modulation of emotional responding to unpleasant pictures: an ERP study. *Psychophysiology* 43: 292–296, 2006. doi:10.1111/j.1469-8986.2006.00402.x.

Näätänen R, Picton TW. N2 and automatic versus controlled processes. *Electroencephalogr Clin Neurophysiol Suppl* 38: 169–186, 1986.

Nieuwenhuis S, Holroyd CB, Mol N, Coles MG. Reinforcement-related brain potentials from medial frontal cortex: origins and functional significance. *Neurosci Biobehav Rev* 28: 441–448, 2004. doi:10.1016/j.neubiorev.2004.05.003.

Olofsson JK, Polich J. Affective visual event-related potentials: arousal, repetition, and time-on-task. *Biol Psychol* 75: 101–108, 2007. doi:10.1016/j.biopsycho.2006.12.006.

Padoa-Schioppa C. Orbitofrontal cortex and the computation of economic value. *Ann NY Acad Sci* 1121: 232–253, 2007. doi:10.1196/annals.1401.011.

Padoa-Schioppa C. Neuronal origins of choice variability in economic decisions. *Neuron* 80: 1322–1336, 2013. doi:10.1016/j.neuron.2013.09.013.

Padoa-Schioppa C, Assad JA. Neurons in the orbitofrontal cortex encode economic value. *Nature* 441: 223–226, 2006. doi:10.1038/nature04676.

Pascual-Marqui RD, Michel CM, Lehmann D. Low resolution electromagnetic tomography: a new method for localizing electrical activity in the brain. *Int J Psychophysiol* 18: 49–65, 1994. doi:10.1016/0167-8760(84)90014-X.

Patel SH, Azzam PN. Characterization of N200 and P300: selected studies of the event-related potential. *Int J Med Sci* 2: 147–154, 2005. doi:10.7150/ijms.2.147.

Payzan-LeNestour E, Dunne S, Bossaerts P, O'Doherty JP. The neural representation of unexpected uncertainty during value-based decision making. *Neuron* 79: 191–201, 2013. doi:10.1016/j.neuron.2013.04.037.

Peters J, Büchel C. Neural representations of subjective reward value. *Behav Brain Res* 213: 135–141, 2010. doi:10.1016/j.bbr.2010.04.031.

Picton TW, Bentin S, Berg P, Donchin E, Hillyard SA, Johnson R Jr, Miller GA, Ritter W, Ruchkin DS, Rugg MD, Taylor MJ. Guidelines for using human event-related potentials to study cognition: recording standards and publication criteria. *Psychophysiology* 37: 127–152, 2000. doi:10.1111/1469-8986.3720127.

Plassmann H, O'Doherty J, Rangel A. Orbitofrontal cortex encodes willingness to pay in everyday economic transactions. *J Neurosci* 27: 9984–9988, 2007. doi:10.1523/JNEUROSCI.2131-07.2007.

Plassmann H, O'Doherty JP, Rangel A. Appetitive and aversive goal values are encoded in the medial orbitofrontal cortex at the time of decision making. *J Neurosci* 30: 10799–10808, 2010. doi:10.1523/JNEUROSCI.0788-10.2010.

Polanía R, Krajbich I, Grueschow M, Ruff CC. Neural oscillations and synchronization differentially support evidence accumulation in perceptual and value-based decision making. *Neuron* 82: 709–720, 2014. doi:10.1016/j.neuron.2014.03.014.

Polich J. Updating P300: an integrative theory of P3a and P3b. *Clin Neurophysiol* 118: 2128–2148, 2007. doi:10.1016/j.clinph.2007.04.019.

Raghuraman AP, Padoa-Schioppa C. Integration of multiple determinants in the neuronal computation of economic values. *J Neurosci* 34: 11583–11603, 2014. doi:10.1523/JNEUROSCI.1235-14.2014.

Rangel A, Camerer C, Montague PR. A framework for studying the neurobiology of value-based decision making. *Nat Rev Neurosci* 9: 545–556, 2008. doi:10.1038/nrn2357.

Rolls ET, Grabenhorst F, Parris BA. Neural systems underlying decisions about affective odors. *J Cogn Neurosci* 22: 1069–1082, 2010. doi:10.1162/jocn.2009.21231.

San Martín R. Event-related potential studies of outcome processing and feedback-guided learning. *Front Hum Neurosci* 6: 304, 2012. doi:10.3389/fnhum.2012.00304.

Scherg M, Von Cramon D. Evoked dipole source potentials of the human auditory cortex. *Electroencephalogr Clin Neurophysiol* 65: 344–360, 1986. doi:10.1016/0168-5597(86)90014-6.

Schlereth T, Baumgärtner U, Magerl W, Stoeter P, Treede RD. Left-hemisphere dominance in early nociceptive processing in the human parasylvian cortex. *Neuroimage* 20: 441–454, 2003. doi:10.1016/S1053-8119(03)00345-8.

Smith NK, Cacioppo JT, Larsen JT, Chartrand TL. May I have your attention, please: electrocortical responses to positive and negative stimuli. *Neuropsychologia* 41: 171–183, 2003. doi:10.1016/S0028-3932(02)00147-1.

Stancak A, Hoechstetter K, Tintera J, Vrana J, Rachmanova R, Kralik J, Scherg M. Source activity in the human secondary somatosensory cortex depends on the size of corpus callosum. *Brain Res* 936: 47–57, 2002. doi:10.1016/S0006-8993(02)02502-7.

Stancak A, Johnstone J, Fallon N. Effects of motor response expectancy on cortical processing of noxious laser stimuli. *Behav Brain Res* 227: 215–223, 2012. doi:10.1016/j.bbr.2011.10.018.

Taylor MJ, Smith ML, Iron KS. Event-related potential evidence of sex differences in verbal and nonverbal memory tasks. *Neuropsychologia* 28: 691–705, 1990. doi:10.1016/0028-3932(90)90124-7.

Tom SM, Fox CR, Trepel C, Poldrack RA. The neural basis of loss aversion in decision-making under risk. *Science* 315: 515–518, 2007. doi:10.1126/science.1134239.

Tzovara A, Chavarriaga R, De Lucia M. Quantifying the time for accurate EEG decoding of single value-based decisions. *J Neurosci Methods* 250: 114–125, 2015. doi:10.1016/j.jneumeth.2014.09.029.

Vrána J, Polácek H, Stancák A. Somatosensory-evoked potentials are influenced differently by isometric muscle contraction of stimulated and non-stimulated hand in humans. *Neurosci Lett* 386: 170–175, 2005. doi:10.1016/j.neulet.2005.06.005.

Walsh MM, Anderson JR. Learning from experience: event-related potential correlates of reward processing, neural adaptation, and behavioral choice. *Neurosci Biobehav Rev* 36: 1870–1884, 2012. doi:10.1016/j.neubiorev.2012.05.008.

Weinberg A, Hajcak G. Beyond good and evil: the time-course of neural activity elicited by specific picture content. *Emotion* 10: 767–782, 2010. doi:10.1037/a0020242.

Wilkinson N, Klaes M. *An Introduction to Behavioral Economics*. Basingstoke, UK: Palgrave Macmillan, 2012. doi:10.1007/978-0-230-39103-1.

Wolach I, Pratt H. The mode of short-term memory encoding as indicated by event-related potentials in a memory scanning task with distractions. *Clin Neurophysiol* 112: 186–197, 2001. doi:10.1016/S1388-2457(00)00501-0.

Wright H, Li X, Fallon NB, Giesbrecht T, Thomas A, Harrold JA, Halford JC, Stancak A. Heightened eating drive and visual food stimuli attenuate central nociceptive processing. *J Neurophysiol* 113: 1323–1333, 2015. doi:10.1152/jn.00504.2014.

Yeung N, Cohen JD. The impact of cognitive deficits on conflict monitoring. Predictable dissociations between the error-related negativity and N2. *Psychol Sci* 17: 164–171, 2006. doi:10.1111/j.1467-9280.2006.01680.x.

Yeung N, Sanfey AG. Independent coding of reward magnitude and valence in the human brain. *J Neurosci* 24: 6258–6264, 2004. doi:10.1523/JNEUROSCI.4537-03.2004.

Yu R, Huang Y. A nickel ain't worth a dime anymore: the illusion of money and the rapid encoding of its true value. *PLoS One* 8: e55025, 2013. doi:10.1371/journal.pone.0055025.